Tallimustine Lesions in Cellular DNA are AT Sequence-Specific but Not Region-Specific†

Maryanne C. S. Herzig, Alex V. Trevino, Brenda Arnett, and Jan M. Woynarowski*,‡

Cancer Therapy and Research Center, Institute for Drug Development, 14960 Omicron Drive, San Antonio, Texas 78245

Received June 7, 1999; Revised Manuscript Received August 16, 1999

ABSTRACT: Tallimustine (FCE 24517) is an AT-specific alkylating antitumor derivative of distamycin. This study examined levels of tallimustine lesions in intracellular DNA, their sequence- and region-specificity, and the long-range distribution of the drug binding motif. Tallimustine adducts in DNA converted to strand breaks by heating allowed the quantitation of drug lesions. In bulk DNA of intact human leukemia CEM cells, tallimustine formed 0.15 ± 0.04 and 0.64 ± 0.18 lesions/kbp at 5 and 50 μM, respectively. These lesions represent monoadducts as no interstrand cross-links or DNA−protein cross-links were detected. Tallimustine adducts in intracellularly treated DNA showed a general preference for sequences with T-tracts, suggesting a propensity for intrinsically bent motifs. Major drug-adducted sites identified by repetitive primer extension, included 5′-TTTTGPu-3′ and 5′-TTTTGC-3′ motif. Despite the high specificity at the nucleotide level, tallimustine did not differentiate among bulk DNA and three discrete AT-rich regions of genomic DNA examined by quantitative PCR stop assay with lesion frequencies ranging from 0.23 to 0.39 lesions/kbp at 25 μM drug. In comparisons of lesion frequencies and cytotoxicity, tallimustine adducts are ∼50 times more lethal than relatively nonsequence specific cisplatin adducts but are >100 times less lethal than lesions by an unrelated AT-specific drug, bizelesin. However, the 5′-TTTTGPu-3′ motifs targeted by tallimustine are relatively infrequent and scattered throughout the genome. In contrast, the motifs 5′-T(A/T)$_4$A-3′ motifs targeted by bizelesin, while also infrequent, cluster in defined AT-rich islands. The lack of region-specificity may be the reason tallimustine adducts, despite high AT-specificity at the nucleotide level, are less lethal than region-specific bizelesin adducts.

An intensive research is carried out by many laboratories on the rational design of sequence-specific DNA-reactive drugs that are related to AT-specific netropsin and distamycin (for review see refs *1* and *2*). One such agent, which has reached clinical trials as a broad-spectrum anti-cancer drug, is tallimustine (FCE 24517, Figure 1) (*3*−*6*).

Tallimustine is a hybrid of the antibiotic distamycin and a nitrogen mustard moiety. The distamycin portion can form hydrogen bonds in the minor groove conferring AT-specific sequence recognition and then the nitrogen mustard can alkylate DNA bases (*3*, *4*). Both components seem to contribute to the drug's biological properties as tallimustine is markedly more cytotoxic than either distamycin or simple nitrogen mustards (*3*). Because of the binding through the minor groove, tallimustine alkylates N3 positions of adenine residues (*7*), unlike conventional nitrogen mustards, which typically alkylate N7 positions of guanine residues in the major groove. Both reversible (noncovalent) interactions and irreversible (covalent) adducts were noted with drug-treated naked DNA, including a suggestion of interstrand cross-linking (*8*). Footprinting and various polymerase extension studies confirmed tallimustine binding to AT-rich tracts and established drug binding sites to be 5′-TTTTGA and 5′-TTTTAA (*7*−*11*), while closely related drugs were found to generally prefer the 5′-TTTTGPu sites (*12*, *13*).

Tallimustine binding to cellular DNA and its consequences have been less extensively investigated. Low levels of irreversible, presumably covalent drug adducts were demonstrated with a radiolabeled drug, but no other types of DNA lesions were detected by alkaline elution (*14*). Potentially relevant to the antitumor activities of tallimustine, drug adducts seem to be poorly recognized by cellular DNA-repair systems (*15*). Other studies suggested that significant differences exist in the mechanisms of action of tallimustine and the "classical" nitrogen mustard drugs such as melphalan (*16*−*18*).

In contrast to "classical" alkylating drugs, which tend to target G-clusters (*19*, *20*), tallimustine, as a distamycin derivative, is likely to target AT-rich domains of cellular DNA. Recognition of AT-rich motifs T(A/T)$_4$A appears to be relevant to the antiproliferative properties of another AT-specific, structurally unrelated drug, bizelesin (*21*−*25*). Given the recognition of more discrete sequence motifs, tallimustine has the potential to be even more specific than bizelesin in cellular systems. It remains unknown, however, whether a general AT-preference, targeting of specific AT-rich motifs

† This study was supported in part by a grant from the National Cancer Institute (CA71969) and by CTRC Research Foundation, San Antonio TX.

* To whom correspondence should be addressed. Jan M. Woynarowski, Ph.D., Head, Molecular Pharmacology, Cancer Therapy and Research Center, Institute for Drug Development, 14960 Omicron Dr., San Antonio, TX 78245. Telephone: 210-677-3832. Fax: 210-677-0058. E-mail: jmw1@saci.org.

‡ Preliminary account of this study has been presented in part at the10th NCI-EORTC Symposium on New Drugs in Cancer Therapy, June 16−19, 1998, Amsterdam, Netherlands, Abstract No. 527.

[1] Abbreviations: RPE- repetitive primer extension; PCR-polymerase chain reaction; QPCR-quantitative polymerase chain reaction.

10.1021/bi991286r CCC: $18.00
Published on Web 10/01/1999

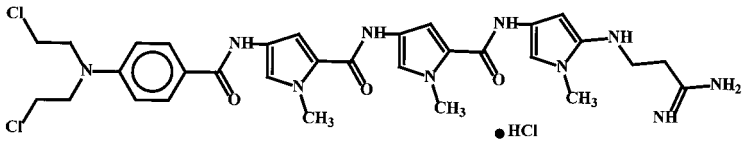

FIGURE 1: Structure of tallimustine.

or regions, or simply binding in the minor groove, are the determinants of tallimustine-induced cell growth inhibition.

In this investigation, we characterized sequence-specificity of tallimustine-induced lesions in intracellular DNA and quantified their frequencies in bulk DNA and in selected specific regions. Our results confirm that tallimustine recognizes highly specific AT-rich motifs and damages AT-rich domains in cellular DNA; however, this high specificity at the nucleotide level is not accompanied by preferential recognition of AT-rich regions, because sequences recognized by tallimustine are relatively infrequent and scattered throughout the genome.

MATERIALS AND METHODS

Chemicals. Tallimustine FCE 24517 was a generous gift from Dr. Enrico Pesenti at Pharmacia & Upjohn (Milan, Italy), and its stock solutions were made in DMSO. Bizelesin, U78779, was generously provided Drs. Patrick McGovren and Robert Kelly at the Pharmacia & Upjohn, Inc. (Kalamazoo, MI), and its stock solutions were made in *N*,*N*-dimethylacetamide. Stock solutions were stored at −20 °C protected from light. SV40 DNA, RPMI 1640, and Joklik's media were from Gibco-BRL, (Gaithersburg, MD). [^{14}C]-Thymidine (59.7 mCi/mmol) was from Dupont NEN (Boston, MA). Agarose was from FMC (Rockland ME). All other chemicals were reagent grade.

Cell Cultures and Cytotoxic Activity. Human CEM leukemia cells (from Dr. William T. Beck, University of Illinois, Chicago) were cultured in suspension using Joklik's medium containing 10% fetal bovine serum (*26*). African green monkey kidney BSC-1 cells (from Dr. Terry Beerman, Roswell Park Cancer Inst., Buffalo, NY) were cultured as described previously (*24*, *27*). When drug effects on intracellular SV40 DNA were examined, cells were infected with SV40 virus as described (*24*, *27*, *28*) and at 40 h postinfection treated with drug for 4 h at 37 °C. SV40 DNA was then isolated as described previously (*28*).

Drug cytotoxic activities against CEM cells were assayed by the standard MTT assay (*20*, *29*). Drug treatment was for 72 h using exponentially growing cells at 1.5×10^3 cells/0.2 mL in a 96-well plate. The absorbance signal for drug-treated and control wells (Tr and Con, respectively) and the initial absorbance (T_0, determined separately) were used to calculate cell growth relative to control as a ratio of (Tr-T_0)/(Con-T_0) and drug concentration inhibiting relative cell growth by 50% (GI_{50}) (*30*).

Tallimustine Damage to Purified SV40 DNA. Tallimustine-induced damage to naked circular SV40 DNA were assessed based on thermal conversion of drug adducts to breaks. Purified SV40 DNA (250 ng in 25 μL of TE (10 mM TRIS-HCl, pH 8.0, 1 mM EDTA)) was incubated for 4 h at 37 °C with the indicated drug concentrations. Aliquots (10 μL) of drug-treated samples were supplemented with 3 μL loading buffer (6 × 15% ficoll, in Tris, (Amressco, Inc., Solon, Ohio)) and heated for 15 min at 95 °C to convert drug adducts to DNA drug breaks. Topological forms were separated by agarose gel electrophoresis, stained with Sybr Green I and photographed. The negatives were scanned in a Molecular Dynamics (San Jose, CA) laser densitometer. The images were processed using Image Quant software (Molecular Dynamics). The heat-induced conversion of Form I (supercoiled DNA) to Form II (relaxed circular), indicating single strand breaks is expressed relative to total Form I initially present. The frequencies of drug lesions were calculated based on Poisson distribution as described elsewhere (*24*).

Tallimustine Total Adducts in Bulk DNA of Intact Cells and Isolated Nuclei. Covalent adducts in genomic DNA of intact cells or isolated nuclei were quantified based on induction of heat-labile sites using the approach similar to that previously described for bizelesin (*24*, *31*), except that single-label and external controls were used. Briefly, CEM cells were incubated overnight with 0.1 μCi/ml of [^{14}C]-thymidine. Cells were harvested, resuspended at 0.5×10^5 cells/mL in a fresh medium for an additional 30 min incubation at 37 °C and incubated with drugs as indicated. After drug treatment, cells were washed with cold PBS by centrifugation at 200*g* for 6 min, resuspended at 1×10^6 cells/mL in 1% Sarkosyl, 1 M NaCl, 10 mM EDTA, pH 8.6, and heated for 15 min at 90 °C, protected from light. Aliquots of cell lysates (150 μL) were loaded onto sucrose gradients (*24*), which consisted of 0.4 mL of 1% Sarkosyl in 2.5% sucrose (lysing solution layer), a 10 mL, 5−20% sucrose layer, and a 0.5 mL, 60% sucrose cushion (all in 2 mM EDTA, 300 mM NaOH, 700 mM NaCl). After loading, gradients were then overlaid with an additional 0.1 mL of lysing solution. After 1 h at 20 °C, gradients were centrifuged at 17 000 rpm (36 500*g*) for 19 h in an SW40Ti rotor (Beckman-Coulter,) followed by the fractionation and processing of gradient fractions as described (*24*, *31*). Frequencies of heat-labile sites (breaks) in genomic DNA were calculated as described previously (*24*, *31*).

An analogous procedure was used for drug treatment of isolated nuclei. Nuclei were isolated from [^{14}C]-thymidine prelabeled cells as described previously (*32*) with minor modifications. Briefly, radiolabeled cells were washed by centrifugation (6 min at 200*g*) in cold PBS and then with a nuclei isolation buffer (2 mM K_2HPO_4/KH_2PO_4, pH 7.0, 5 mM $MgCl_2$, 15 mM NaCl, and 1 mM EDTA) at 4 °C. The cell pellet was resuspended in the same buffer, supplemented with 0.3% (v/v) Triton X-100, and allowed to lyse for 30 min at 4 °C. Nuclei were harvested by centrifugation (300*g*, 10 min) and resuspended in the isolation buffer at 0.5×10^6 nuclei/mL. After drug treatment, nuclei suspensions were diluted with the isolation buffer and centrifuged (300*g*, 13 min). The pellets were resuspended at 1×10^6 nuclei/mL in 1% Sarkosyl, 1 M NaCl, 10 mM EDTA, pH 8.6. Further steps were identical as described for intact cells.

Interstrand Cross-Links in Drug-Treated Nuclei by Alkaline Sucrose Gradient Centrifugation. The ability of talli-

mustine to induce interstrand cross-links was assessed by an alkaline sucrose gradient sedimentation as described elsewhere (*25*), except that isolated nuclei were used instead of intact cells. Nuclei were isolated, treated with drugs, and subjected to sedimentation analysis as described above for total adducts with the following exceptions. Nuclei harvested after drug treatment were resuspended in the isolation buffer and loaded without heating on alkaline sucrose gradients. After a 10 h lysis at 20 °C, gradients were centrifuged at 17 000 rpm (36500*g*) for 11 h at 20 °C in an SW41Ti rotor.

Sites of Drug Adducts—Repetitive Primer Extension (RPE). Localization of tallimustine adducts was determined with linear amplification of DNA fragments prematurely terminated during primer extension on a drug-modified DNA template (*20, 25*). To analyze drug adducts in intracellular SV40 DNA, SV40 virus-infected BSC-1 cells were treated with tallimustine or bizelesin for 4 h. SV40 DNA was isolated as described (*24, 27, 31*) and used in the RPE reactions (see below).

Primers to be used in RPE were 5′-end-labeled and purified as described (*20, 25*). Sequences of these primers and their positions in SV40 sequence were given elsewhere (*25*). Primers complementary to SV40 bottom and top strand were denoted with a suffix "U" and "L", respectively.

RPE reactions (20 μL) typically consisted of 1× buffer II, 1.5 mM $MgCl_2$, 0.2 mM of each dNTP, 1U *Taq* polymerase (all PCR Core Reagents, Perkin-Elmer, Norwalk, CT), 1.25 μM end-labeled primer, and 0.1 μg template SV40 DNA (*20, 25*). Thermal cycling, performed in a model 9600 Thermal Cycler (Perkin-Elmer), used the following conditions: for the NO system: 95 °C for 30 s, followed by 30 cycles of 94 °C for 15 s, 55 °C for 30 s, and 60 °C for 45 s; for the ORI system, 95 °C for 30 s, followed by 30 cycles of 94 °C for 15 s, 40 °C for 20 s, and 69 °C for 25 s; for the MAR2 system, 95 °C for 30 s, followed by 30 cycles of 94 °C for 15 s, 55 °C for 30 s, and 72 °C for 15 s. The final cycle was followed by an extra 6 min of extension at 72 °C. Sequencing reactions were performed with the same primer as in the RPE reactions, using Sequenase v.2 (Amersham, Piscataway, NJ) and [^{35}S] dATP (1000 Ci/mmol, 12.5mCi/mL, NEN, Boston, MA). Equal volume aliquots of each RPE reaction (usually 2 μL) were analyzed on 8% polyacrylamide/urea sequencing gels along with the sequencing reactions. Following electrophoresis, autoradiography, and imaging (*20, 25*), the positions of drug-induced stop sites were determined based on these sequencing ladders run in the same gel. Drug adducts are assumed to be within $\pm 1-2$ bp from the positions of stop sites (*25*).

Quantitative Polymerase Chain Reaction (QPCR) Stop Assay. QPCR on drug-treated DNA was performed essentially as described previously (*20, 22*). CEM cells were prelabeled with [^{14}C]-thymidine and treated with drug as described above for total adducts. Following drug treatment, cells were washed by centrifugation with PBS and their DNA was extracted and purified using PureGene (Gentra Systems, Minneapolis, MN). PCR reactions were carried out in triplicate at two different levels of template DNA (based on ^{14}C radioactivity) and were set up using PCR core reagents (Perkin-Elmer) with 0.05 mM dGTP and 0.04 μCi/reaction of [^{32}P]dGTP (NEN).

The following primer systems and cycling conditions were used. For a 743-bp region in the *c-myc* ORI domain, 5′-GCCGTTTTAGGGTTTGTTG-3′ and 5′-CAAAAAACATTCTTCTCATCC-3′ were used as the upper and lower primer, respectively. PCR was carried out with initial denaturation at 95° for 30 s, followed by 20 cycles of 94° for 15 s, 55° for 30 s, and 68° for 30 s. For a 947-bp region in the *c-myc* MAR domain, 5′-CCAAGCAGAGGAGCAAAA-3′ and 5′-AGGGGACTGGCACTGGTTA-3′ were used as the upper and lower primer, respectively. PCR was carried out with initial denaturation at 95° for 30 s, followed by 20 cycles of 94 °C for 15 s, 55° for 30 s and 68 °C for 20 s. For a 1025-bp region in an AT-rich island domain, (a portion of GenBank sequence Z79699), 5′- TATTATTGTATCATGAG-GGT-3′ and 5′-ACTCCGTTTTAATTAGTTAT-3′ were used as the upper and lower primer, respectively. PCR was carried out with initial denaturation at 95 °C for 30 s, followed by 23 cycles of 94 °C for 20 s, 55 °C for 30 s and 68 °C for 45 s. For all the systems, terminal extension was performed at 68 °C for 3−10 min. Following electrophoresis in 1% agarose and autoradiography, signal intensities were quantified in a Molecular Dynamics densitometer. Amplification inhibition data were converted to lesion frequency using a Poisson distribution formula and the frequency data were expressed as lesions/Kbp/μM drug (*20*).

Analysis of Drug Binding Motifs. The distribution of drug-binding motifs was analyzed in over $>20 \times 10^6$ bp of human sequences from GenBank using a custom Msearch program (generously provided by Dr. Stephen Hardies at the University of Texas Health Science Center, San Antonio, TX) and a template programmed in Visual Basic in Excel spreadsheet (Microsoft, Redmond, WA). This search provided a number of hits for specified binding motifs in each 250 bp section ("bin") of the analyzed sequences and cataloged all the analyzed entries based on the maximal number of hits per bin. Examples of the results are presented in Figure 7 as histograms of hits along the position in DNA sequence using "bins" of 250 bp.

RESULTS

Thermal Conversion of Tallimustine-DNA Adducts to Strand Breaks. Previous studies suggested that adducts by tallimustine are thermally labile (*8, 14, 15*). A similar thermal lability of various N3 adenine adducts is a convenient feature to determine and quantify total DNA adducts by other drugs (*24, 27, 31*). However, thermally inducible breaks have not been used thus far to estimate the frequency of tallimustine adducts.

To validate this approach and establish the conditions for quantitative conversion of tallimustine adducts to breaks, we utilized drug-treated naked SV40 DNA. Strand breakage in this system was followed based on the topological forms conversion. A single strand break effects the conversion of supercoiled Form I to relaxed circular Form II (Figure 2), whereas double strand breaks would result in conversion to linear Form III. After a 4 h drug treatment with tallimustine at 37 °C and followed by 15 min at 95 °C, the percentage of Form I is drastically reduced with increasing tallimustine concentration. Prolonged heating did not result in a further decrease in Form I (data not shown). When drug lesions were calculated based on Poisson distribution (*24, 33*), $\sim$ 0.16 lesions/kbp at 10 μM tallimustine was identified. This value

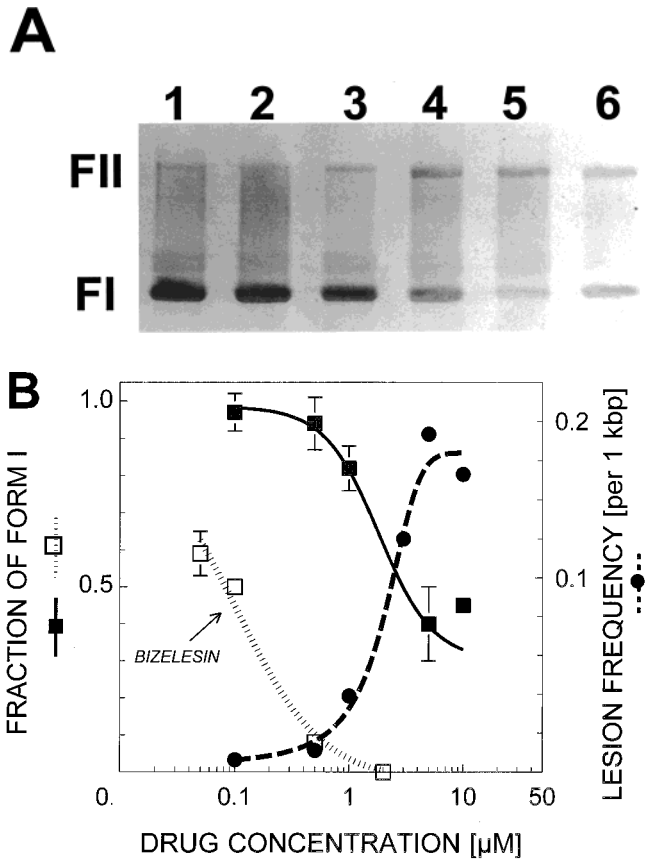

FIGURE 2: Induction of thermally labile adducts by tallimustine in naked SV40. Panel A. Representative agarose electrophoresis of SV40 DNA incubated for 4 h at 37 °C with tallimustine at 0 μM (lanes 1), 0.2 μM (lane 2), 0.5 μM (lane 3), 1.0 μM (lane 4), and 5.0 μM (lane 5) or with bizelesin at 0.05 μM (lane 6). Samples were heated for 15 min at 95 °C prior to electrophoresis to convert drug adducts to strand breaks. The positions of supercoiled Form I and relaxed Form II of SV40 DNA are indicated. The proportions of Form I and II in unheated drug-treated samples did not differ from those in control samples (not shown). Panel B. Quantitation of thermally labile adducts based on the topological forms conversion after 4 h incubation of SV40 DNA with drugs. The topological conversion of Form I, expressed relative to total Form I initially present, for tallimustine (solid lines, ■) and bizelesin (dotted line, □) are shown. The results are averaged values (±SE) from 2 to 3 independent experiments. The frequency of tallimustine lesions (dashed line, ●) was calculated from the topological forms conversion data based on Poisson distribution (*24*).

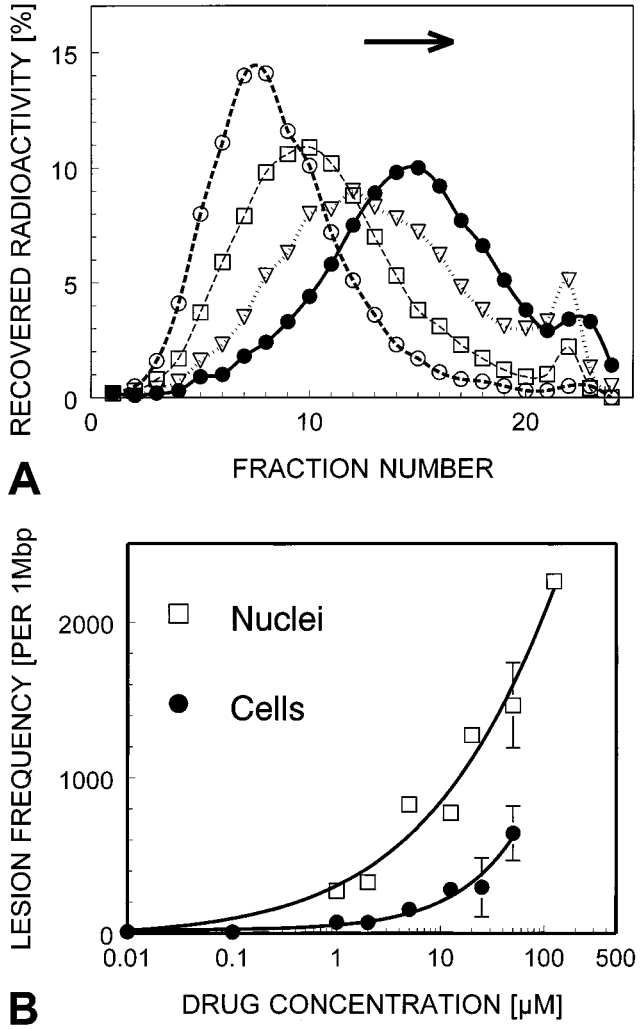

FIGURE 3: Thermally labile adducts by tallimustine in DNA from drug-treated intact CEM cells or isolated CEM nuclei. Panel A. Sedimentation profiles of DNA from intact cells treated for 4 h with 0 (●), 5 (▽), 12.5 (□), or 50 (○) μM tallimustine. Lysates from drug-treated [^{14}C]-thymidine prelabeled cells were heated at 95 °C for 15 min prior to sedimentation in alkaline sucrose gradients. Slower sedimenting DNA from tallimustine-treated cells indicates heat-induced breaks resulting from drug adducts. Panel B. Quantitation of thermally labile tallimustine adducts in intact cells and isolated nuclei. The frequencies of drug lesions were derived from experiments such as in Panel A were calculated as previously described for both isolated nuclei (□) and intact cells (●).

compares with 1×10^{-4}/bp/h reported by Fontana (*8*) at 2.5 μM tallimustine in salmon sperm DNA. Another adenine-reactive drug, bizelesin, was used as a positive control and produced a similar effect, although at markedly lower concentrations.

Tallimustine Lesions in Human Genomic DNA in Nuclei and Intact Cells. Having established the utility of thermally inducible breaks for the quantitation of tallimustine-DNA adducts, we next used this approach for genomic DNA. Thus, we quantified the heat-labile sites as a measure of drug lesions in bulk DNA of both isolated nuclei and intact CEM cells. In both situations, thermally induced strand breaks in genomic DNA were monitored based on shifts in the sedimentation profiles of tallimustine-treated samples. In these experiments, [^{14}C]-thymidine prelabeled cells or nuclei were drug-treated for 4 h at 37 °C, lysed, and heated at 95 °C for 15 min to convert tallimustine adducts to strand breaks prior to analysis by sedimentation in alkaline sucrose gradients. Slower sedimenting DNA from tallimustine-treated cells indicates heat-induced breaks resulting from drug adducts. As illustrated by representative sedimentation profiles, incubation of intact CEM cells with increasing drug concentration leads to increased DNA strand breaks manifested as the progressive shifts of the sedimentation profiles toward the top of the gradients (Figure 3A).

The frequencies of drug-adducted sites were calculated as previously described (*24*, *31*) from several experiments for both drug-treated cells and isolated nuclei and are summarized in Figure 3B. For both intact cells and in isolated nuclei, these lesion frequencies are clearly dependent on drug concentration. For example, treatment of cells with tallimustine at 5, 12.5, and 50 μM resulted in 150, 280, and 640 lesions/Mbp. Isolated nuclei are markedly more sensitive to tallimustine than whole cells.

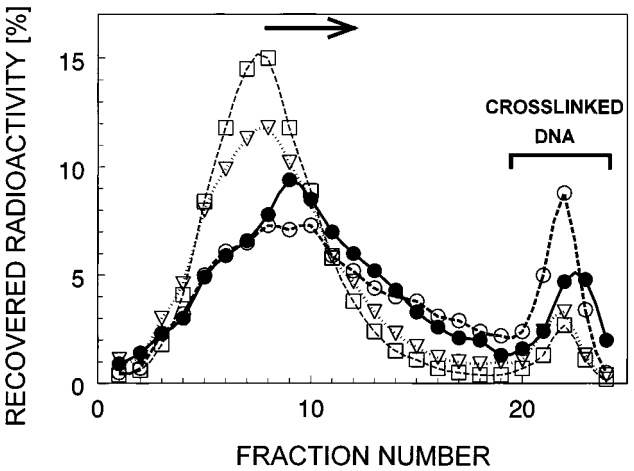

FIGURE 4: The lack of interstrand cross-links in tallimustine-treated nuclei from CEM cells. Nuclei isolated from cells pre-labeled with [^{14}C]thymidine were treated with 0 (●), 50 (▽), and 125 (□) μM tallimustine or with 0.05 (○) μM Bizelesin for 4 h and then subjected to sedimentation through strand separating alkaline sucrose gradients. No increase in the fastest sedimenting fraction, the cross-linked fraction, is seen with tallimustine.

Lack of Induction of Interstrand Cross-Links or DNA−Protein Cross-Links by Tallimustine in Human Genomic DNA. The benzoic acid mustard moiety of tallimustine is potentially capable of forming cross-linked adducts. The ability of tallimustine to cross-link genomic DNA was directly investigated in the nuclei of CEM cells prelabeled with [^{14}C]-thymidine. Nuclei were treated with increasing concentrations of tallimustine or bizelesin for 4 h and then subjected to sedimentation on alkaline sucrose gradients (without prior heating, i.e., without converting adducts to breaks, Figure 4). Under these conditions, monoadducts should not affect DNA sedimentation, whereas interstrand cross-linking would prevent alkali-induced strand separation resulting in the appearance of a rapidly sedimenting, larger DNA. An increase in the material sedimenting near the bottom of the gradient is seen for 0.05 μM bizelesin, which serves as a positive control for cross-link induction. Tallimustine, however, shows no increase in rapidly sedimenting material above control levels even at a very high drug concentration of 125 μM. If anything, sedimentation profiles from tallimustine-treated nuclei suggested a slight reduction in DNA size, possibly reflecting direct (as opposed to heat-induced) strand breaks at these very high concentrations. Given that 125 μM tallimustine produced numerous adducts (cf. Figure 3), data in Figure 4 demonstrate that these drug adducts do not include detectable cross-links.

Additional experiments demonstrated also that tallimustine does not induce DNA−protein cross-links as found by the technique of K^+/SDS precipitation (*25, 26*). The marginal (0.9%) fraction of DNA coprecipitated with proteins in cells treated with up to 50 μM tallimustine compared to 0.8% for control cells and contrasted with the ∼85% for cells incubated with 50 μM formaldehyde (data not shown).

Tallimustine Sites in Intracellular SV40. The sites of tallimustine adducts in intracellular DNA were mapped in a model system of SV40 virus infected cells, which has proved useful in our previous studies of DNA adducts of bizelesin and related drugs (*23−25, 27*). Intracellular SV40 DNA in virus-infected cells maintains chromatin organization, like genomic DNA, but provides much more abundant target sequence than genomic sequences, which facilitates lesion analysis. To map tallimustine adducts in SV40 DNA from virus-infected and drug-treated cells, we used repetitive primer extension (RPE). In this assay, linear amplification of drug-modified template by *Taq* polymerase generates nascent strands, which are prematurely terminated by adducts on template strands. (*20, 25*).

Tallimustine forms highly specific lesions in intracellularly drug-treated SV40 DNA. Figure 5A shows examples of RPE data for the upper and lower strands of NO regions serving as templates along with the sequencing lanes used to identify the positions of the stop sites. The reactions with untreated (control) SV40 DNA resulted mainly in extension products, which migrate near the top of the gel, i.e., which are longer than the few hundred bp resolved on the gel (lanes 1−2). In contrast, samples with drug-treated DNA showed several distinct bands corresponding to shorter, prematurely terminated, nascent strands (lanes 3−6). Generation of these prematurely terminated extension products coincides with the gradual abrogation of the very long products. Within a window of appropriate drug concentrations (e.g., 5−20 μM), although the overall signal intensity varied, the banding pattern remained similar (Figure 5A, lanes 4−6). For drugs such as bizelesin, high drug levels can abrogate primer extension completely (data not shown). Bizelesin adducts, while formed at only a limited number of sites, can eliminate the majority of SV40 molecules as templates for longer products (Figure 5A, lane 3, upper portion of gel).

Sequencing reactions with the same primers enable the localization of stop sites with the resolution of 1−2 bp (*20, 25*). Table 1 shows the adduct sites identified using primers for three different SV40 regions. Fifteen adduct sites were positively identified when over 1400 bp were scanned using three different primer sets. Even the weakest sites identified showed concentration dependence with tallimustine. Of the four strongest drug-adduct sites identified, three conformed to the consensus sequence of 5′-TTTTGPu-3′, designated type "A" in Figure 5A and in Table 1. Wherever this sequence occurred, an adduct was found. The other previously reported binding motif 5′-TTTTAA-3′, also designated type "A" (*7, 11*) was scarce in the three SV40 regions examined. Of three sites with this sequence, one is strongly adducted, one is not. The adduction status of the third 5′-TTTTAA-3′ site could not be determined due to its localization in an area of the gels with significant band compression (Figure 5A). The other strong site 5′-TTTTTGC-3′, type "B", was also an atypical bizelesin site. Nonclassical yet relatively strong sites were seen at 5′-ATTTGPu-3′ and 5′-AGTTGPu-3′, type "C". Among other moderate to weak sites such as 5′-CTTTGG-3′, 5′-ATTTGT-3′, and 5′-AATTGT-3′, type "D", the minimum shared motif seemed to be TTG. Another moderate site, 5′-TTTTTAC-3′, type "E", was shared with bizelesin. These results show that the consensus sequence previously established for tallimustine with naked DNA represents the main sites, although not all sites, of adducts with intracellular DNA.

Interestingly, nonconsensus sites were observed opposite consensus sites when both strands were mapped by RPE. Although weak, the atypical sites, designated "F" in Figure 5A, were consistently present (Figure 5B). These two nonconsensus sites were observed on the upper template as a multisite at 5′-CCCCAAA-3′ (position 2044−2046) and a

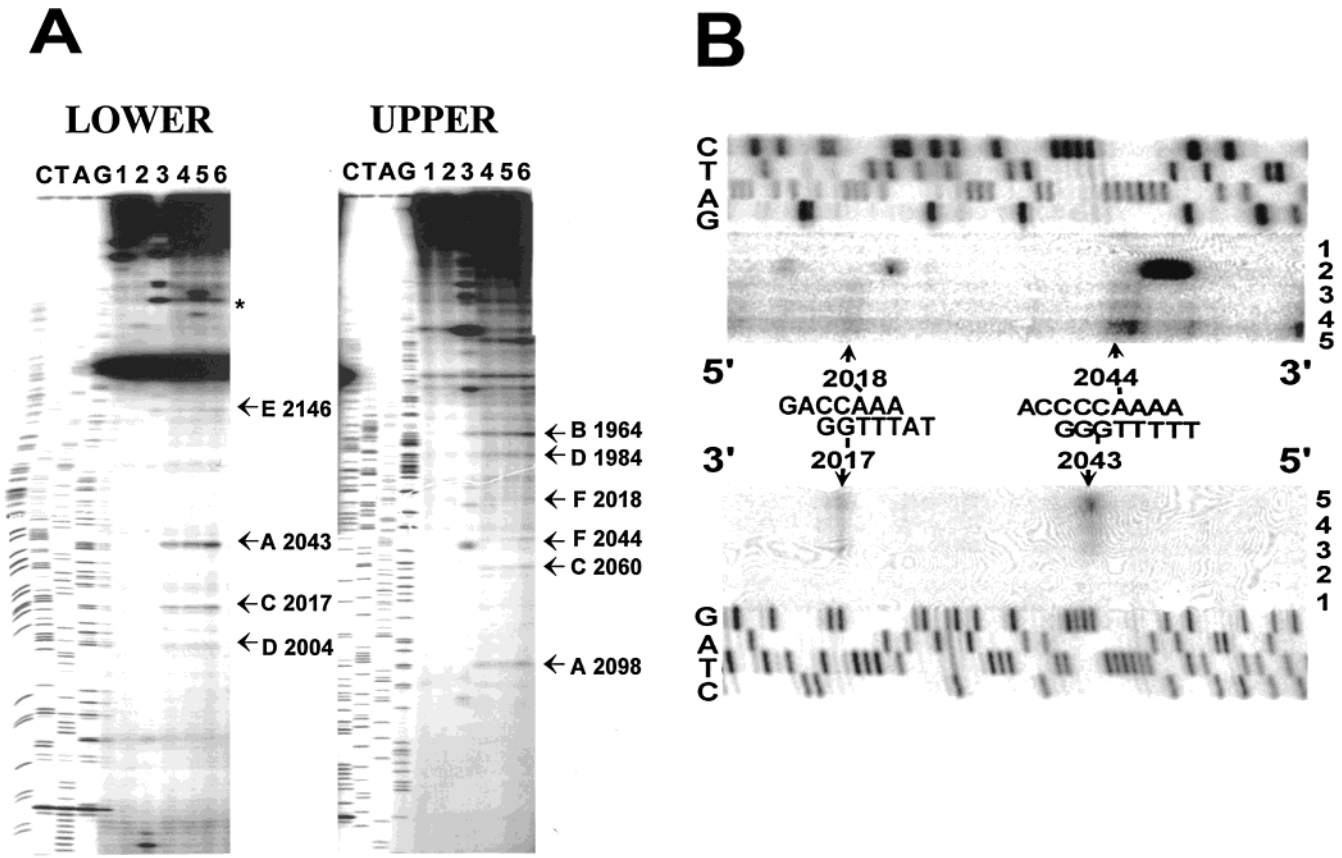

FIGURE 5: Sites of tallimustine adducts in intracellular SV40 DNA. BSC-1 cells infected with SV40 were treated with drug for 4 h, and drug adducts in isolated plasmid DNA were mapped using Repetitive Primer Extension (see Materials and Methods for details). Primer extension on drug-modified DNA is prematurely terminated opposite drug-adducts in the template strands. Panel A. Representative gel with both upper and lower primers. A sequencing gel is shown with the leftmost lanes from sequenase reactions, designated C T A G, denoting bases in the template strand. RPE reactions for SV40 DNA from control (nondrug-treated) cells (lanes 1−2), and cells treated with bizelesin at 5 μM (lane 3) and tallimustine at 5, 10, and 20 μM (lanes 4−6) are shown. Tallimustine-specific stop sites are marked with both position and type designation (see Table 1). All the marked sites reproducibly appeared in at least two independent experiments, and include a range of sites from very strong, typical sites (type A) to very weak, atypical sites (type F). The stop site marked with an asterisk is in a region of band compression and appears to be around site 2366. Panel B. Weak atypical tallimustine sites (type F) and the adjacent strong sites (types A and C) on the complementary strand. Weak adducts at nonconsensus sites, type F at 2044 and 2018 are opposite stronger sites on the duplex strand, type A at 2043 and type C at 2017. Sequencing lanes for each primer are designated C T A G. Control (nondrug-treated) (lanes 1); Bizelesin at 5 μM (lane 2) and Tallimustine at 5, 10, and 20 μM (lanes 3−5) treated DNA are shown. This is an enlargement from an experiment similar to that in Panel A.

weaker site at 5′-GACCAA-3′ (position 2018) and are opposite strong consensus sites on the complementary strand (positions 2043 and 2017, respectively).

Tallimustine Lesions in Specific Regions of Genomic DNA vs Bulk-DNA Lesions. Given the high sequence-specificity of tallimustine lesions at the nucleotide level, it was possible that the drug could differentially damage various regions in the genome with a preference for AT-rich loci. Therefore, tallimustine lesions were quantified in specific AT-rich regions of genomic DNA from drug-treated CEM cells by QPCR stop assay. In this method, drug lesions on the DNA template interfere with primer extension, resulting in decreased amplification of a target region (*20, 26*). The selected regions included two domains of known function in the *c-myc* gene, MAR and ORI, as well as an AT-rich island of unknown function but with MAR properties, identified by us in GenBank entry Z79699. (Figure 6).

Tallimustine inhibits amplification of each of the three regions examined (Figure 6). The inhibition, however, is incomplete even at 25 μM, suggesting a limited number of available sites and/or limited drug reactivity. Conversion of amplification data to lesion frequencies indicate no significant differences among the analyzed regions, although the relatively less AT-rich domain, *c-myc* ORI, seems to be marginally less affected by tallimustine (Table 2). Also, the similar values suggest that tallimustine-induced lesions in the selected regions show no preference over bulk DNA. For example, 25 μM of the drug produced 0.3 lesions/kbp in bulk DNA and 0.23−0.31 in the specific regions.

In contrast to weak amplification inhibition by tallimustine, a profound inhibition is caused by bizelesin at sub-micromolar concentrations (Figure 6) consistent with previous studies (*21*) and the higher overall reactivity of equimolar bizelesin with bulk DNA (Table 2). Importantly, unlike tallimustine, bizelesin showed severalfold higher lesion frequencies in certain AT-rich loci than in bulk DNA (Table 2 and ref *21*).

DNA Lesions and Cytotoxicity. To assess the potential of tallimustine-induced DNA lesions for cell growth inhibition, we related drug cytotoxicity to the estimated lesion frequencies and compared tallimustine to AT-specific, bizelesin, and a relatively nonspecific drug, cisplatin. Per equimolar concentrations, tallimustine forms similar levels of DNA adducts as cisplatin. In comparison to bizelesin, however,

Table 1: Examples of Tallimustine Adduct Sites in SV40 DNA from Drug-Treated BSC-1 Cells Derived from Several RPE Gels Like Those Shown in Figure 5

	adduct sites in intracellular SV40 DNA				
				position in SV40 sequence[a]	
	motif designation[b]	intensity (arbitrary)	sequence[c]	lower strand	upper strand
A	typical	very strong	5′-TTTTGPu-3′	2043 5197[d]	2098
			5′-TTTTAA−3′	5148[d]	
B	atypical	very strong	5′-TTTTGC-3′		1964
C	typical	strong to moderate	5′-ATTTGPu-3′	2017; 4125	2060
			5′-AGTTGPu-3′		
D	atypical	moderate to weak	5′-CTTTGG-3′		1984
			5′-ATTTGT−3′	4149	
			5′-AATTGT-3′	4173	
			5′-GTTTGC-3′	2004	
E	atypical	moderate	5′-TTTTAC-3′	2146	
F	atypical with site on the complementary strand	weak	5′-CCCCAAA-3′		2044
			3′-g ***g*** t t t t-5′	(*2043*)	
			5′-GACCAA-3′		2018
			3′-g **g** t t t a-5′	(*2017*)	

[a] Stop site position in the SV40 sequence refers to a residue across from the last 3′ nucleotide in nascent chain, resulting in stop bands such as those in Figure 5. A relative position of +1 toward the 5′ end is most likely to correspond to the adducted base, although adducts may be located up to 1−2 bases from the stop site. Site position in general was verified from at least two separate experiments. [b] Typical motif corresponds to 5′-TTTTGPu-3′ or 5′-TTTTAA-3′ previously reported as tallimustine consensus sequence with naked DNA (*7, 10, 12, 13*). [c] Capital letters correspond to the likely drug binding sites inferred from stop sites (underlined) assuming the adducted base to be within ±1−2 bp from the stop site (*25*).[d] Site position determined from single gel. In type F sites, the sequence in small letters denotes strong stop site on complementary strand.

tallimustine induced, per μM of drug, 45-fold fewer lesions in bulk DNA. The differences between the two drugs were even more pronounced for region-specific lesions with tallimustine being 75- to 420-fold less reactive (Table 2 and ref *21*).

The respective cytotoxic activities of tallimustine, bizelesin, and cisplatin, tested in the human leukemic cell line CEM (Table 2), were even more divergent than lesion frequencies. With the GI_{50} values of 3.5 nM, 0.6 pM and 1.5 μM, respectively, tallimustine was less cytotoxic than bizelesin by nearly 6000-fold and more cytotoxic than cisplatin by ~430-fold. These differences cannot be explained solely by different DNA reactivities.

The extrapolation of drug reactivities with cellular DNA (lesions/kbp/μM values in Table 2) to their respective GI_{50} concentrations shows that equitoxic levels of tallimustine, bizelesin, and cisplatin result in widely different levels of DNA lesions. These estimates suggest that nearly 220 DNA lesions (adducts) by tallimustine are required per cell for 50% growth inhibition, as opposed to only 2 DNA lesions/cell by bizelesin (Table 2). Thus, tallimustine adducts seem to be over 100-fold less cytotoxic than bizelesin adducts. Still, tallimustine lesions appear ~50-fold more cytotoxic than cisplatin lesions, since the latter drug forms an estimated ~14,000 lesions at its GI_{50} concentration (Table 2). Being derived from the simplistic linear extrapolation of the detected lesion frequencies, these estimates should not be over-interpreted. Nevertheless, they suggest profound differences in the "lethality" of DNA lesions by tallimustine, bizelesin, and cisplatin.

Long-Range Sequence Analysis for Drug-Binding Motifs. To further explore the DNA sequence aspect of the differences among tallimustine, bizelesin, and cisplatin, we analyzed human DNA sequences for the distribution of respective binding motifs. The results of this search, which covered $>20.1 \times 10^6$ bp, are summarized in Table 3 and the examples of motif distribution in selected loci are shown in Figure 7.

Consistent with the most stringent sequence, the tallimustine motif 5′-TTTTGPu-3′ is approximately 10 and 170 times less frequent than motifs for bizelesin and cisplatin, respectively. Moreover, these infrequent tallimustine sites are distributed more or less uniformly throughout the genome. The maximal number of hits found for tallimustine in the entire search was 4−5 per 250 bp section and was similar to the high hits in an average GenBank entry analyzed.

Similar, a nearly uniform pattern is shown by cisplatin motifs, except that all the scored hits are markedly higher than for tallimustine, proportional to the greater overall abundance of cisplatin motifs. In contrast to the uniformly scattered tallimustine and cisplatin motifs, the bizelesin motif, while being infrequent in the majority of regions, forms clusters in several loci. In these clusters, local bizelesin "motif density" exceeds severalfold the maximal hits in an average locus (Table 3, Figure 7).

DISCUSSION

Tallimustine is one of the most sequence-specific small molecular weight anticancer drugs. In this study, we verify that tallimustine is capable of inducing highly specific DNA lesions in AT-tracts of intracellular DNA. In addition to sequence preferences at the nucleotide level, the nature of these lesions, their levels, and the potential of targeting specific regions of genomic DNA are assessed.

The frequencies of total tallimustine DNA lesions were estimated based on the conversion of adducts to breaks upon heating. This approach has been validated with naked DNA yielding results that are comparable to previous estimates using other methods. For instance, approximately 0.16 lesions/kbp in naked SV40 DNA at 10 μM tallimustine was identified. This value is comparable to 1×10^{-4}/bp/h

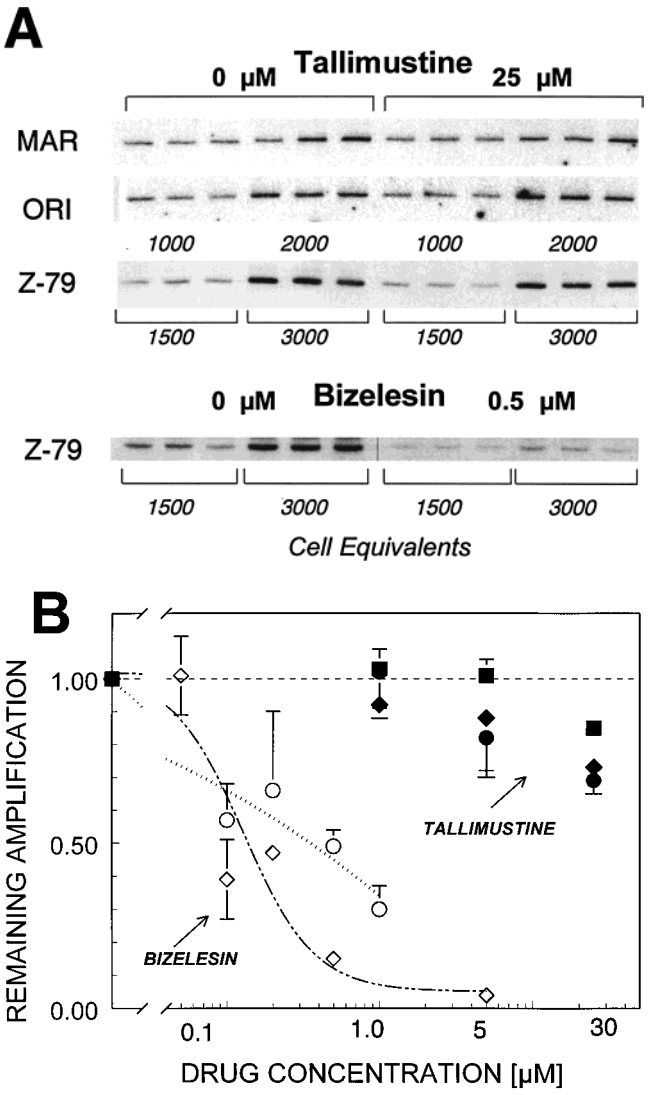

FIGURE 6: Tallimustine lesions in specific regions of cellular DNA. CEM cells were treated with drugs for 4 h; their DNA was isolated, quantified, and subjected to QPCR. Panel A. Examples of agarose electrophoresis of amplified DNA from: control cells and cells treated with 25 μM tallimustine using primers for c-myc MAR, c-myc ORI, and an AT-rich island domain identified in GenBank entry Z79699, and control cells and cells treated with 0.5 μM bizelesin using primers for the Z79699 system. The determinations were carried out in triplicate using two different DNA amounts (expressed as cell equivalents). Panel B. Quantitation of region-specific DNA damage. Amplification normalized relative to the amplification of DNA from control cells (relative amplification) is plotted for DNA from tallimustine-treated cells (solid symbols) and bizelesin-treated cells (open symbols) using primers for c-myc MAR (●○), c-myc ORI (■), and Z79699 (◆◇) regions. The data represent average values (±SE) from 2 to 3 independent experiments performed as in the examples shown in Panel A.

covalent adducts reported by Fontana (*8*) at 2.5 μM tallimustine in salmon sperm DNA.

In intact CEM cells, tallimustine forms ~0.03 lesions/kbp/μM. This lesion frequency is comparable to the values quantified by Broggini et al. using radiolabeled drug (*14*). For instance, 248.5 pmols tallimustine/μg DNA (equivalent to ~ 0.39 adducts/kbp) was reported after a 1 h incubation of L1210 cells with 12.5 μM of the drug (*14*). Intact nuclei are more sensitive than whole cells, probably reflecting the elimination of a drug uptake barrier. Cellular uptake of tallimustine, distamycin, and its analogues, in general, is known to be poor and drug availability in intact cells is limited (*14*). On a molar basis, the overall frequency of tallimustine adducts in bulk genomic DNA resembles that of typical alkylating drugs such as cisplatin, although tallimustine is less reactive with both naked and genomic DNA than another AT-specific drug, bizelesin.

Monoadducts are the prevailing, if not the only, type of lesions induced by tallimustine in genomic DNA. Interstrand cross-links, while theoretically possible, have been ruled out as a significant type of lesion. There was no evidence of cross-linking by a sensitive technique of alkaline gradient sedimentation analysis in nuclei treated with up to 125 μM tallimustine. Tallimustine also does not form DNA−protein cross-links. These results corroborate the lack of cross-links in cellular DNA suggested by alkaline elution data (*14*). It remains unknown why tallimustine, unlike other nitrogen mustard drugs, is unable to form significant numbers of cross-links. Possibly, steric constraints resulting from drug binding in the minor groove prevent the second arm reaction of the nitrogen mustard group.

High preference for AT-rich sites with a definite consensus sequence is clearly a hallmark of tallimustine binding to DNA. Of the four strongest drug-adduct sites identified, by repetitive primer extension, three conformed to the consensus sequence of 5′-TTTTGPu-3′. One such site, 5′-TTTTTGC-3′, was also an atypical bizelesin site. In addition, tallimustine adducts were found with all of the evaluated 5′-TTTTGPu-3′ sites (3/3). In contrast, adduction at the 5′-TTTTAA-3′ sequence was observed only in one of two evaluated instances of that motif. Consistent with previous reports with naked DNA (*7*, *34*, *35*), other factors than the narrowly defined motif sequence determine whether 5′-TTTTAA-3′ motif is adducted by tallimustine.

Among other moderate to weak sites, the minimum shared motif seemed to be 5′-TTG-3′. Nonconsensus sites included a multisite at 5′-CCCCAAA-3′ as well as a weaker site at 5′-GACCAA-3′ and were found opposite strong consensus sites on the complementary DNA strand. Such overlapping adduct sites might reflect GG or GA interstrand cross-links. However, this contrasts with the lack of significant tallimustine cross-links in genomic DNA. It cannot be ruled out that a strong binding to one strand somehow impedes primer extension on the complementary strand. Alternatively, the overlapping sites may reflect two independent monoadducts on different DNA molecules.

The A-tracts in all the major tallimustine-binding sites suggest that the drug prefers bent DNA. $(A)_n$-tracts are known to bend DNA toward the minor groove to a degree that depends on the number of consecutive adenine residues (*36*−*38*). Distamycin, the prototype molecule for tallimustine also with a preference for A/T-sites, causes DNA bending through the widening of the minor groove (*39*, *40*), the opposite effect of narrowing the minor groove by the $(A)_n$-tracts. Thus, distamycin effectively unbends intrinsically bent sequences (*39*). Distamycin-induced change in the bend status of drug-binding site may affect protein binding in the vicinity as suggested for transcription factors (inhibition) (*41*) or topoisomerase II (stimulation by low concentrations of distamycin) (*42*, *43*). Similar unbending of bent $(A)_n$-tracts can be expected for tallimustine−DNA adducts. Thus, it is possible that the distortion of local DNA bending may play a role in cellular effects of tallimustine.

Table 2: Cytotoxicity, Region-Specific, and Bulk-DNA Lesions Induced by Tallimustine and Bizelesin in CEM Cells

drug	cytotoxicity[a] GI_{50} [M]	lesions in:	lesions/Kbp at 25 μM drug[b]	lesions/ Kbp/μM	estimated lesions/cell at GI_{50}[h]
tallimustine	3.5×10^{-9}	bulk DNA	0.30	0.022[c]	220
		AT-island in GenBank Z79699	0.31	0.012[d]	
		c-myc MAR	0.39	0.016[d]	
		c-myc ORI	0.23	0.009[d]	
bizelesin	0.6×10^{-12}	bulk DNA	ND	0.88[e]	2
		AT-island in GenBank Z79699	ND	5.5[f]	
		c-myc MAR	ND	1.86[f]	
cisplatin	1.5×10^{-6}	bulk DNA	ND	0.032[g]	14000

[a] Determined by the MTT assay. [b] Bulk DNA data from Figure 3, region-specific data based on Figure 6. [c] An average value for 5−25 μM tallimustine (based on data in Figure 3). [d] The value for 25 μM tallimustine in Figure 6. [e] An average value for 0.1−0.4 μM bizelesin (*21*). [f] An average value for 0.1−0.5 μM and 0.2−1 μM bizelesin for Z79699 and c-myc MAR, respectively (based on data in Figure 6 and (*21*)). [g] Based on data in (*45*). [h] Estimated by linear extrapolation of lesion frequencies/Kbp/μM to the GI_{50} concentration assuming 2.9×10^9 bp/cell (rounded values).

Table 3: Long-Range Sequence Analysis for the Distribution of Possible Drug Binding Sites[a]

drug	motif searched	average hits/ 250 bp (±SD)[a]	maximal hits/250 bp/ in average GenBank entry[b]	maximal hits/ 250 bp in "hot" loci[c]
tallimustine	TTTTGPu	0.3 ± 0.6	2.8	4−5
bizelesin	$T(A/T)_4A$	2.8 ± 3.6	19	30−99
cisplatin[d]	GG, GNG, GC	50.5 ± 13.7	97	97−154

[a] A comparison of tallimustine with an unrelated AT-specific drug, bizelesin, and with a relatively nonspecific drug, cisplatin. [b] The total of 387 GenBank entries covering >20.1 Mbp of human DNA sequences were analyzed. The "hits" recorded include overlapping, i.e., mutually exclusive, sites and are given as average values per 250 bp sequence sections ("bins", cf. Figure 7). [c] Average of maximal hits per 250 bp sequence sections ("bins") found in each GenBank entry scored (unweighted for length differences of individual entries). [d] Maximal hits/250 bp sequence sections ("bins") in the highest scoring loci. [e] Because of large number of "hits", the data for cisplatin are based on a subset of sequences totaling 2.72 Mbp, except for the average hits value which is based on the full 20.1 Mbp dataset.

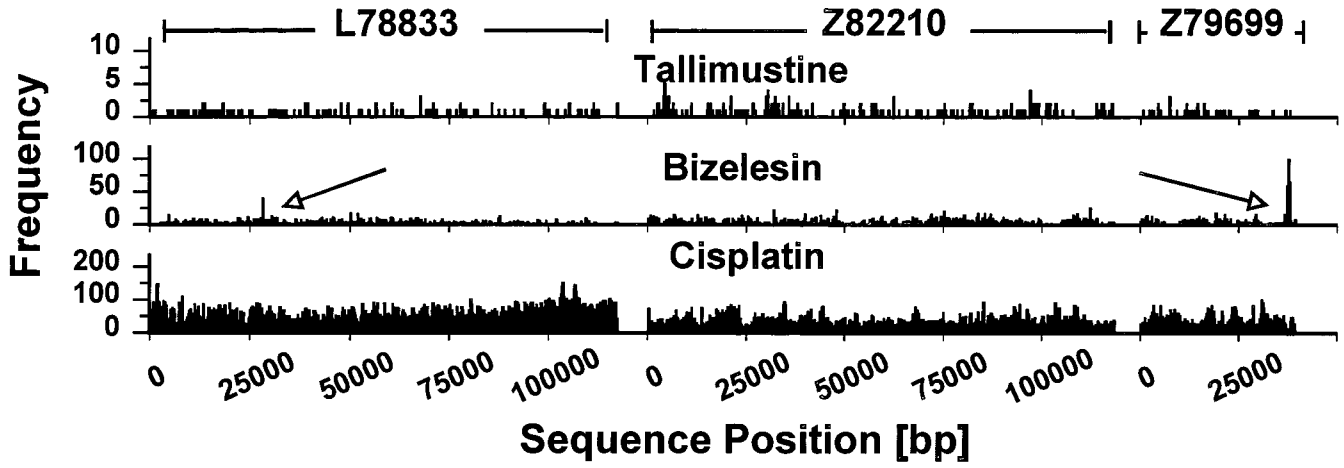

FIGURE 7: Distribution histogram of drug binding motifs in human genome for tallimustine (TTTTGPu), bizelesin, $T(A/T)_4A$, and cisplatin (Pt-motif: GG, GNG, GC). The ordinate shows the number of motif occurrences (including mutually exclusive positions) per "bins" of 250 bp along the sequence. The figure depicts motif distribution in two GenBank entries (out of the total analyzed 3878 entries of ~20.1 Mbp). These sequences represent a typical region for tallimustine binding (L78833) and a region with the highest identified "density" of tallimustine motifs (Z82210). Note different Y scales for various motifs.

Comparison of tallimustine and an unrelated AT-specific drug, bizelesin, emphasizes potentially critical aspects for sequence- and region-specific drug targeting. Both drugs preferentially alkylate the N3 atom of purine residues in the minor groove (*7*, *34*, *35*). Both drugs have distinct but not entirely dissimilar DNA binding specificities for AT-rich motifs; tallimustine prefers 5′-TTTTGPu-3′, while bizelesin prefers 5′-$T(A/T)_4A$-3′ tracts. Despite these similarities and the high specificity, however, tallimustine does not differentiate among bulk DNA and several discrete AT-rich regions of genomic DNA examined by QPCR stop assay.

Unlike tallimustine, bizelesin shows preferential recognition of specific regions. Consistent with differential damage observed by QPCR, the bizelesin motif is generally infrequent but clusters in several AT-rich loci, resulting in the spikes of a local "motif density" that exceed many times the highest values in an average analyzed GenBank entry. In contrast, the tallimustine motif shows uniformly low "density" throughout the genome, which can be the main reason tallimustine exhibits no preference for the examined AT-rich regions. The scattered and infrequent tallimustine sites, while highly specific at the nucleotide level, paradoxi-

cally resemble the distribution of relatively nonspecific sites for cisplatin. Thus, at a resolution of a few hundred bp, both tallimustine and cisplatin bind throughout, except that tallimustine forms infrequent and cisplatin very frequent lesions.

The targeted motifs and their distribution, i.e., region specificity, may play a role in the relative lethality of drug-induced lesions. AT-specific tallimustine lesions seem to be markedly more cytotoxic (~50-fold) than GC-specific cisplatin adducts. On the other hand, tallimustine lesions are clearly less cytotoxic than bizelesin lesions, perhaps by as much as 2 orders of magnitude. The likely explanation for this difference is that hits in regions preferentially targeted by bizelesin are more critical to cell survival than scattered hits by tallimustine. An alternative explanation could be that lesions formed by tallimustine, i.e., monoadducts, represent an inherently less cytotoxic type of DNA damage than interstrand cross-links, which correspond to at least 30−40% of DNA lesions by bizelesin (*25*). This possibility, however, seems less likely, since it is inconsistent with the lower lethality of lesions by cisplatin, with an estimated 3−25% of DNA lesions being interstrand cross-links (*44*, *45*).

In summary, tallimustine forms highly AT-specific monoadducts in intracellular DNA with a strong preference for intrinsically bent sequences such as 5′-TTTTGPu-3′. High specificity of tallimustine sequence recognition may be a factor in its cytotoxic effects, although it does not lead to a significant region specificity and less sequence-specific adducts by bizelesin are markedly more lethal. Thus, a drug's ability to affect a critical region with several lesions resulting from clusters of binding motifs, as is the case with bizelesin, can be more important than just sequence-specificity at the nucleotide level. We show that drug sequence-specificity can be used to reliably predict region specificity. In light of our results, it seems critical to include the notion of region-specificity in the strategies aimed at the design of sequence-specific drugs.

ACKNOWLEDGMENT

We thank Drs. Randy Wadkins and Daekyu Sun for their critical review of the manuscript.

REFERENCES

1. Walker, W. L., Kopka, M. L., and Goodsell, D. S. (1997) *Biopolymers 44*, 323−334.
2. Bailly, C., and Chaires, J. B. (1998) *Bioconjugate Chem. 9*, 513−38.
3. Arcamone, F. M., Animati, F., Barbieri, B., Configliacchi, E., R, D. A., Geroni, C., Giuliani, F. C., Lazzari, E., Menozzi, M., and Mongelli, N. (1989) *J. Med. Chem. 32*, 774−8.
4. Pezzoni, G., Grandi, M., Biasoli, G., Capolongo, L., Ballinari, D., Giuliani, F. C., Barbieri, B., Pastori, A., Pesenti, E., Mongelli, N., and et al. (1991) *Br. J. Cancer 64*, 1047−50.
5. Punt, C. J., Humblet, Y., Roca, E., Dirix, L. Y., Wainstein, R., Polli, A., and Corradino, I. (1996) *Br. J. Cancer 73*, 803−4.
6. Viallet, J., Stewart, D., Shepherd, F., Ayoub, J., Cormier, Y., DiPietro, N., and Steward, W. (1996) *Lung Cancer 15*, 367−73.
7. Broggini, M., Coley, H. M., Mongelli, N., Pesenti, E., Wyatt, M. D., Hartley, J. A., and D'Incalci, M. (1995) *Nucl. Acids Res. 23*, 81−7.
8. Fontana, M., Lestingi, M., Mondello, C., Braghetti, A., Montecucco, A., and Ciarrocchi, G. (1992) *Anti-Cancer Drug Des. 7*, 131−41.
9. Broggini, M., Ponti, M., Ottolenghi, S., D'Incalci, M., Mongelli, N., and Mantovani, R. (1989) *Nucl. Acids Res. 17*, 1051−9.
10. Wyatt, M. D., Garbiras, B. J., Haskell, M. K., Lee, M., Souhami, R. L., and Hartley, J. A. (1994) *Anti-Cancer Drug Des. 9*, 511−25.
11. Beccaglia, P., Grimaldi, K. A., Hartley, J. A., Marchini, S., Broggini, M., and D'Incalci, M. (1996) *Br. J. Cancer 73*, 12.
12. Brooks, N., Lee, M., Wright, S. R., Woo, S., Centioni, S., and Hartley, J. A. (1997) *Anti-Cancer Drug Des. 12*, 591−606.
13. Brooks, N., Hartley, J. A., Simpson, J. E. Jr., Wright, S. R., Woo, S., Centioni, S., Fontaine, M. D., McIntyre, T. E., and Lee, M. (1997) *Bioorg. Med. Chem. 5*, 1497−507.
14. Broggini, M., Erba, E., Ponti, M., Ballinari, D., Geroni, C., Spreafico, F., and D'Incalci, M. (1991) *Cancer Res. 51*, 199−204.
15. Rossi, R., Montecucco, A., Capolongo, L., Mezzina, M., Chevallier-Lagente, O., Sarasin, A., and Ciarrocchi, G. (1996) *Anticancer Res. 16*, 3779−83.
16. Coley, H. M., Mongelli, N., and D'Incalci, M. (1993) *Biochem. Pharm. 45*, 619−26.
17. Geroni, C., Pesenti, E., Tagliabue, G., Ballinari, D., Mongelli, N., Broggini, M., Erba, E., D'Incalci, M., Spreafico, F., and Grandi, M. (1993) *Int. J. Cancer 53*, 308−14.
18. Erba, E., Mascellani, E., Pifferi, A., and D′Incalci, M. (1995) *Int. J. Cancer 62*, 170−5.
19. Mattes, W. B., Hartley, J. A., Kohn, K. W., and Matheson, D. W. (1988) *Carcinogenesis 9*, 2065−72.
20. Woynarowski, J. M., Chapman, W. G., Napier, C., Herzig, M., and Juniewicz, P. (1998) *Mol. Pharm. 54*, 770−777.
21. Woynarowski, J. M., Hardies, S. C., Trevino, A., and Arnett, B. (1998) in *10th NCI-EORTC Symposium on New Drugs in Cancer Therapy, Amsterdam, June 16−19*, pp Abstract 528., Amsterdam.
22. Woynarowski, J. M., Napier, C., and W., C. (1997) *Proc. Am. Assoc. Cancer Res. 38*, 228.
23. Woynarowski, J. M., and Beerman, T. A. (1997) *Biochim. Biophys. Acta 1353*, 50−60.
24. Woynarowski, J. M., McHugh, M., Gawron, L. S., and Beerman, T. A. (1995) *Biochemistry 34*, 13042−13050.
25. Woynarowski, J. M., Chapman, W. G., Napier, C., and Herzig, M. C. S. (1999) *Biochim. Biophys. Acta 1444*, 201−217.
26. Woynarowski, J. M., Napier, C., Koester, S. K., Chen, S.-F., Troyer, D., Chapman, W., and MacDonald, J. R. (1997) *Biochem. Pharm. 54*, 1181−93.
27. McHugh, M. M., Woynarowski, J. M., Mitchell, M. A., Gawron, L. S., Weiland, K. L., and Beerman, T. A. (1994) *Biochemistry 33*, 9158−68.
28. Grimwade, J. E., Cason, E. B., and Beerman, T. A. (1987) *Nucl. Acids Res. 15*, 6315−29.
29. Arnould, R., Dubois, J., Abikhalil, F., Libert, A., Ghanem, G., Atassi, G., Hanocq, M., and Lejeune, F. J. (1990) *Anticancer Res. 10*, 145−154.
30. Monks, A., Scudiero, D., Skehan, P., Shoemaker, R., Paull, K., Vistica, D., Hose, C., Langley, J., Cronise, P., Vaigro-Wolff, A., and et al. (1991) *J. Natl. Cancer Inst. 83*, 757−66.
31. Zsido, T. J., Woynarowski, J. M., Baker, R. M., Gawron, L. S., and Beerman, T. A. (1991) *Biochemistry 30*, 3733−8.
32. Woynarowski, J. M., McCarthy, K., Reynolds, B., Beerman, T. A., and Denny, W. A. (1994) *Anticancer Drug Des. 9*, 9−24.
33. Roberts, J. J., and Friedlos, F. (1981) *Biochim. Biophys. Acta 655*, 146−51.
34. D'Incalci, M., Broggini, M., Damia, G., and Erba, E. (1995) in *EORTC Early Drug Development Meeting*, pp 23, Corfu, Greece.
35. Wyatt, M. D., Lee, M., Garbiras, B. J., Souhami, R. L., and Hartley, J. A. (1995) *Biochemistry 34*, 13034−41.
36. Koo, H. S., Drak, J., Rice, J. A., and Crothers, D. M. (1990) *Biochemistry 29*, 4227−34.
37. Nadeau, J. G., and Crothers, D. M. (1989) *Proc. Natl. Acad. Sci. U.S.A. 86*, 2622−6.

38. Haran, T. E., Kahn, J. D., and Crothers, D. M. (1994) *J. Mol. Biol. 244*, 135−43.
39. Barcelo, F., Muzard, G., Mendoza, R., Revet, B., Roques, B. P., and Le Pecq, J. B. (1991) *Biochemistry 30*, 4863−73.
40. Luck, G., Zimmer, C., Reinert, K. E., and Arcamone, F. (1977) *Nucl. Acids Res. 4*, 2655−70.
41. Kim, J., Klooster, S., and Shapiro, D. J. (1995) *J. Biol. Chem. 270*, 1282−8.
42. Woynarowski, J. M., McHugh, M., Sigmund, R. D., and Beerman, T. A. (1989) *Mol. Pharmacol. 35*, 177−82.
43. Fesen, M., and Pommier, Y. (1989) *J. Biol. Chem. 264*, 11354−9.
44. Plooy, A. C., Fichtinger-Schepman, A. M., Schutte, H. H., van Dijk, M., and Lohman, P. H. (1985) *Carcinogenesis 6*, 561−6.
45. Woynarowski, J. M., Trevino, A. V., Arnett, B., Faivre, S., Chaney, S., Vaisman, A., and Varchenko, M. (1999) *Proc. Am. Assoc. Cancer Res. 40*, Abstract 1951.

BI991286R